Biochimica et Biophysica Acta, 980 (1989) 371–376
Elsevier

BBA 74402

A fluorescent probing study on microenvironments in bile salt micelles and bile salt/phosphatidylcholine mixtures in the absence or presence of cholesterol

Katsumi Matsuzaki, Isao Yokoyama, Hiroaki Komatsu, Tetsurou Handa and Koichiro Miyajima

Faculty of Pharmaceutical Sciences, Kyoto University, Sakyo-ku (Japan)

(Received 18 October 1988)

Key words: Microenvironment; Bile salt; Phosphatidylcholine; Cholesterol; Pyrene; Thiacarbocyanine

Microenvironments (micropolarities and microviscosities) in bile salt micelles (sodium cholate, sodium deoxycholate, sodium taurocholate, and sodium glycocholate), sodium taurocholate/egg yolk phosphatidylcholine (egg PC) mixtures, and the above micelles and mixtures containing cholesterol were investigated systemetically by using two fluorescent probes, pyrene and 3,3′-dioctadecyl-2,2′-thiacarbocyanine bromide ($C_{18\text{-}18}$). The vibr[illegible] structure of pyrene fluorescence is a measure of the micropolarities, while the absorption maximal wave number and the fluorescence yield of $C_{18\text{-}18}$ both the micropolarities and the microviscosities. The estimated microenvironments were interpreted in terms of structural variations of these assemblies with the lipid composition and the resultant translocation of the probes. The bile salt micelles were found to have a nonpolar and rigid interior. In the taurocholate/egg PC mixed micelles, the egg PC molecules were motionally more restricted than in egg PC liposomes. The incorporation of cholesterol resulted in a fluidization of the taurocholate micellar interior but a rigidification of the egg PC molecules in the case of the mixed micelles.

Introduction

Bile salts and bile salt/phosphatidylcholine systems are of physiological importance in the intestinal absorption of dietary lipids and in the formation of cholesterol gallstones. Bile salts are amphiphilic in nature and form micelles in aqueous media [1–4]. The micellization process is characteristic of 'mild cooperativity' [5] because of small aggregation numbers, although the size and the shape of the micelles are known to depend on pH, bile salt concentration, and the presence of added salts [1]. Mixed micelles are formed by solubilizing small amounts of phosphatidylcholine and transforming to mixed vesicles [6–11] when the intramicellar fraction of phosphatidylcholine exceeds a critical value. The structures of these assemblies have been extensively investigated by X-ray diffraction [6], quasi-elastic light scattering [7,8], NMR [9], and differential scanning calorimetry [10] techniques.

The locus of a solubilizate in micelles and vesicles is not determined by its structure alone, but the solubilizate–assembly interactions. The solubilized states can, therefore, vary with changes of assembly composition and structure, e.g., the mixed micelle–vesicle transition. The spectral properties of a solubilized optical probe provide some important information on intermolecular interactions between the probe and the surrounding lipids. Thus, polarity (micropolarity) and fluidity (microviscosity) in the close vicinity of the probe molecule (microenvironment) can be evaluated by analysis of the spectral properties of the probe. Many works have been done on microenvironments in 'typical' micelles and vesicles for elucidating the natures of lipid–lipid and lipid–water interactions through the probe–assembly interactions. In contrast, only a few groups have reported on the microenvironments of bile salts and bile salt/phosphatidylcholine systems, suggesting nonpolar and rigid environment within the bile salt micelles [12–16]. These results by different methods for various systems cannot be compared with each other. There

Abbreviations: egg PC, egg yolk L-α-phosphatidylcholine; $C_{18\text{-}18}$, 3,3′-dioctadecyl-2,2′-thiacarbocyanine bromide; SDS, sodium dodecyl sulfate; HED, hepta(ethyleneglycol)dodecyl ether; NaTC, sodium taurocholate.

Correspondence: K. Miyajima, Faculty of Pharmaceutical Sciences, Kyoto University, Sakyo-ku, Kyoto 606, Japan.

have been no systematic studies on the microenvironments in these systems using a single method.

In this work, bile salt micelles, bile salt-phosphatidylcholine mixed micelles and vesicles, and those assemblies containing cholesterol are investigated by using two fluorescence probes, pyrene [17] and 3,3′-dioctadecyl-2,2′-thiacarbocyanine bromide ($C_{18\text{-}18}$) [18]. The microenvironments experienced by the probe molecules in the mixed lipid systems are estimated and interpreted in relation to structural variations with the lipid composition and consequent locus changes of the solubilized probe molecules. Also, a distinction between the bile salt systems and the typical micellar systems is discussed.

Materials and Methods

Materials

Sodium cholate, sodium deoxycholate, sodium glycocholate, and sodium taurocholate were purchased from Nacalai Tesque (Kyoto, Japan). Egg yolk L-α-phosphatidylcholine (egg PC) and cholesterol were obtained from Sigma and Wako (Tokyo, Japan), respectively. Sodium dodecyl sulfate (SDS) from Wako was purified as described previously [19]. Hepta(ethyleneglycol)dodecyl ether (HED) was a product of Nikko Chemicals (Tokyo, Japan). Pyrene from Wako and $C_{18\text{-}18}$ from the Japan Research Institute for Photosensitizing Dye Co. (Okayama, Japan) were used as received. Water was distilled twice from quartz.

Sample preparation

Pyrene or $C_{18\text{-}18}$ was solubilized into micelles and vesicles by a coprecipitation method. A chloroform solution of either dye was mixed in a test tube with a methanol solution of a bile salt and/or a chloroform solution of the lipids (egg PC and/or cholesterol). The solvent was removed with a rotary evaporator, and the residue was dried under vacuum at least 24 h. Then a 15 mM Tris-HCl/135 mM NaCl (pH 7.0) buffer was added and the solution was vortexed. In the case of egg PC-containing vesicle systems, nitrogen gas was purged and then the tube was sealed and left standing for 48 h at room temperature for equilibration [11]. The final concentrations of pyrene and $C_{18\text{-}18}$ were 5 μM and 0.5 μM, respectively.

Spectroscopic measurements

The fluorescence spectra of the pyrene- and $C_{18\text{-}18}$-containing samples were recorded on a Jasco FP-550 spectrofluorimeter at excitation wavelengths of 335 and 530 nm, respectively. Both excitation and emission slit widths were 5 nm. Absorption spectra on a Shimadzu UV-240 spectrophotometer were also measured for the $C_{18\text{-}18}$-solubilized samples. A relative fluorescence quantum yield, ϕ_f^R, was calculated as reported elsewhere [18,21]. Evaluation of ϕ_f^R requires the absorbance of monomeric $C_{18\text{-}18}$ at the excitation wavelength (A_m^{ex}) because of the nonfluorescent property of the dimer. The A_m^{ex} values of the monomer was estimated as follows. At the excitation wavelength, an observed absorbance A_{ex} is expressed as

$$A_{ex} = \varepsilon_m^{ex} C_m + \varepsilon_d^{ex} (C_t - C_m)/2 \quad (1)$$

where ε_m^{ex} and ε_d^{ex} are the molar absorption coefficients of the monomer and the dimer. C_t and C_m are total and monomeric $C_{18\text{-}18}$ concentrations. A similar equation holds at an absorption maximum wavelength.

$$A_{max} = \varepsilon_m^{max} C_m + \varepsilon_d^{max} (C_t - C_m)/2 \quad (2)$$

From Eqns. 1 and 2, one obtains

$$A_m^{ex} = \varepsilon_m^{ex} C_m = \{A_{ex} - (\varepsilon_d^{ex}/\varepsilon_d^{max}) A_{max}\} / \{1 - (\varepsilon_d^{ex}/\varepsilon_d^{max})(\varepsilon_m^{max}/\varepsilon_m^{ex})\} \quad (3)$$

Here we have eliminated C_t to avoid an improperly estimated ϕ_f^R value due to an error in C_t. We have assumed that the spectral shape of the monomer and that of the dimer are the same as those of 3,3′-diethylthiacarbocyanine dye in water [22], except for some wavelength shifts. Thus, by using the values of $\varepsilon_d^{ex}/\varepsilon_d^{max} = 1.82$ and $\varepsilon_m^{ex}/\varepsilon_m^{max} = 0.44$, the absorbance due to the monomer was estimated. This approximation seems to be valid because when [bile salts] > 20 mM (completely monomeric solubilization of $C_{18\text{-}18}$ in the micelles), the monomer absorbances (A_m^{ex}) evaluated from Eqn. 3 are equal to observed A_{ex} values.

All measurements were carried out at 25 ± 0.5 °C.

Results

Pyrene in bile salt micelles

The fluorescence vibronic structure of a pyrene monomer is known to be sensitive to medium polarity [17]. Two fluorescence intensity ratios, I_3/I_1 and I_5/I_1, can be used to monitor microenvironments in the close vicinity of pyrene molecules [13,17]. Here I_1, I_3, and I_5 are the fluorescence intensities of vibronic peaks at about 376, 385, and 394 nm, respectively [17]. These ratios were measured in a series of solvents of graded polarity, i.e., *n*-hexane, 1-octanol, 1-butanol, 1-propanol, ethanol, and methanol, and found to be a monotonously decreasing function with an increasing solvent dielectric constant as a measure of polarity (data not shown). The micropolarities of pyrene in the bile salt micelles were estimated on the basis of the relationship between the intensity ratios and the dielectric constant.

Fig. 1 shows changes of I_3/I_1 and I_5/I_1 as a function of the sodium cholate concentration. The ratios

TABLE I

Microenvironments surrounding pyrene and $C_{18\text{-}18}$ in various micelles and vesicles

Pyrene (5 μM) or $C_{18\text{-}18}$ (0.5 μM) was solubilized in various micelles and vesicles in a 10 mM Tris-HCl/135 mM NaCl buffer (pH 7.0) at 25 °C. The effective dielectric constant (D_{eff}) around pyrene was estimated from the fluorescence intensity ratios (I_3/I_1 and I_5/I_1). The effective dielectric constant (D_{eff}) and the effective viscosity (η_{eff}) experienced by $C_{18\text{-}18}$ were evaluated on the basis of the absorption maximal wave number ($\bar{\nu}_{max}$) and the relative yield (ϕ_f^R). See text.

System	Pyrene			$C_{18\text{-}18}$			
	I_3/I_1	I_5/I_1	D_{eff}	$\bar{\nu}_{max}$ (10^4 cm^{-1})	ϕ_f^R	D_{eff}	η_{eff} (cP)
Sodium cholate micelle	1.39	1.42	7	1.776	12.2	20	39
Sodium deoxycholate micelle	1.52	1.50	5	1.774	13.7	18	106
Sodium taurocholate micelle	1.22	1.30	11	1.774	12.9	18	50
Sodium glycocholate micelle	1.27	1.34	10	1.778	10.8	21	19
SDS micelle	0.97	1.13	22	1.777 [a]	8.4 [a]	18 [a]	9 [a]
HED micelle	0.94	1.12	23	1.776 [a]	6.2 [a]	20 [a]	5 [a]
Egg PC vesicle	1.03	1.22	17	1.779	8.6	22	10
Dipalmitoylphosphatidylcholine vesicle	–	–	–	1.776 [a]	12.3 [a]	21 [a]	63 [a]

[a] From Ref. 21.

increase, and therefore the micropolarity decreases, gradually around 10 mM, suggesting the mild cooperativity [5] of micellar formation. From the constant ratios above 20 mM, one can obtain the micropolarity surrounding pyrene incorporated into the micelle. The micropolarity is expressed in corresponding solvent dielectric constant, termed 'effective dielectric constant' by Mukerjee and Ray [20]. The effective dielectric constant, D_{eff}, (an averaged value from the two ratios) is listed in Table I with values in the other bile salt micelles and typical micelles, i.e., SDS and HED. The D_{eff} values in the bile salt micelles are lower than those in the typical micelles. The order of D_{eff} is sodium deoxycholate < sodium cholate < sodium glycocholate < sodium taurocholate, coinciding with the order of the hydrophilicity of the bile salt molecule itself.

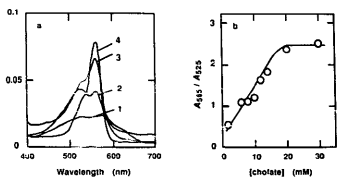

Fig. 2. Changes of the solubilized state of $C_{18\text{-}18}$ with the sodium cholate concentration. $C_{18\text{-}18}$ (0.5 μM) was present in the same system as in Fig. 1. (a) The visible absorption spectra of $C_{18\text{-}18}$ at cholate concentrations (mM) of (1) 2, (2) 6, (3) 10 and (4) 30. (b) Absorbance ratio, A_{565}/A_{525}, as a measure of monomer-to-dimer ratio, plotted against the cholate concentration.

$C_{18\text{-}18}$ in bile salt micelles

We have shown [18,21] that the maximum absorption wave number ($\bar{\nu}_{max}$) of $C_{18\text{-}18}$ is dependent on medium polarity and that its relative fluorescence quantum yield (ϕ_f^R) depends on medium viscosity as well as polarity. On the basis of this dependence, the micropolarity (D_{eff}) and the microviscosity (expressed as "effective

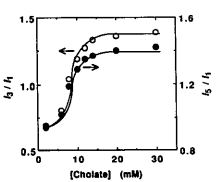

Fig. 1. Changes of the intensity ratios of pyrene fluorescence with the sodium cholate concentration. Pyrene (5 μM) was solubilized in various concentrations of sodium cholate solutions in a 10 mM Tris-HCl/135 mM NaCl (pH 7.0) buffer at 25 °C. Two fluorescence intensity ratios plotted, I_3/I_1 (open circles) and I_5/I_1 (closed circles) are sensitive to medium polarity. See text.

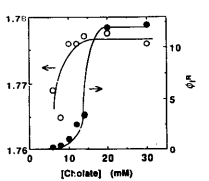

Fig. 3. Variations of the spectral properties of $C_{18\text{-}18}$ as a function of the sodium cholate concentration. The experimental conditions are exactly the same as in Fig. 2. Open circles, the absorption maximal wave number ($\bar{\nu}_{max}$); closed circles, the relative fluorescence yield (ϕ_f^R).

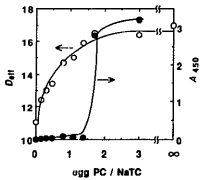

Fig. 4. Micropolarities of pyrene in sodium taurocholate/egg PC mixtures. Pyrene (5 μM) was incorporated in taurocholate/egg PC mixed systems (total lipid concentration, 30 mM) in the buffer at 25°C. Effective dielectric constant (D_{eff}, open circles) estimated from the intensity ratios of pyrene fluorescence is shown as a function of the egg PC-to-taurocholate molar ratio (egg PC/NaTC). Optical absorbance at 450 nm (closed circles) is also plotted as a mark of the micelle-to-vesicle transition.

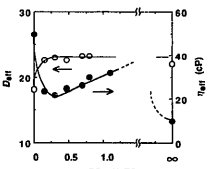

Fig. 5. Microenvironments around $C_{18\text{-}18}$ in sodium taurocholate/egg PC mixtures. $C_{18\text{-}18}$ (0.5 μM) was solubilized in taurocholate/egg PC mixed micelles (total lipid concentration was 30 mM) and in egg PC sonicated vesicles in the buffer at 25°C. Effective dielectric constant (D_{eff}, open circles) and effective viscosity (η_{eff}, closed circles) evaluated from the absorption maximal wave number and the fluorescence yield of $C_{18\text{-}18}$ are plotted against the egg PC-to-taurocholate molar ratio (egg PC/NaTC). The dotted line shows a plausible maximal viscosity in the micelle-to-vesicle transition region.

viscosity", η_{eff}) of the $C_{18\text{-}18}$ fluorophore in micelles and vesicles can be estimated.

Fig. 2a illustrates variation of the $C_{18\text{-}18}$ absorption spectra upon solubilization into sodium cholate micelles. At a low concentration of 2 mM, $C_{18\text{-}18}$ is present mainly as the dimer. An increase in cholate concentration leads to appearance of a monomeric peak around 565 nm. An absorbance ratio, A_{565}/A_{525}, is plotted in Fig. 2b as a measure of the monomer-to-dimer ratio. Here again, the ratio is constant above 20 mM, suggesting complete monomeric solubilization of $C_{18\text{-}18}$. Fig. 3 demonstrates $\bar{\nu}_{max}$ and ϕ_f^R as a function of the cholate concentration. Similar results were obtained for the other bile salts. The $\bar{\nu}_{max}$ and ϕ_f^R values of monomeric $C_{18\text{-}18}$ in the four bile salt micelles as well as in some other micelles and vesicles having alkyl chains are summarized in Table I with the corresponding D_{eff} and η_{eff} values. The D_{eff} values in the bile salt micelles are almost equal to those in the spherical micelles and vesicles, whereas the η_{eff} values are several times higher than those in SDS and HED, and comparable to the microviscosity of the gel-state bilayer (dipalmitoylphosphatidylcholine).

Pyrene in sodium taurocholate / egg PC system

Addition of egg PC to sodium taurocholate micelles causes a gradual increase in and a subsequent leveling-off of pyrene micropolarity, as shown in Fig. 4. The plateau region (egg PC/NaTC > 1.5) is just the same as the vesicular region, which is consistent with an increased turbidity (optical absorbance at 450 nm). Furthermore, the D_{eff} value in the plateau region is equal to that in egg PC vesicles. Here we describe the mixed lipid system in terms of the whole composition, not the assembly composition. The latter, which seems to be a more appropriate expression, may be approximately estimated by using the free taurocholate concentration data in a similar experimental condition (Fig. 15 of Ref. 7). Indeed, the micelle-vesicle boundary (egg PC/NaTC ≈ 1.5) is in accordance with that reported by Mazer et al. (Fig. 9 of Ref. 7).

$C_{18\text{-}18}$ in sodium taurocholate / egg PC micelle

Addition of a small amount of egg PC to sodium taurocholate micelles results in a shift of D_{eff} from 18 to 23 (Fig. 5), the latter value being characteristic of $C_{18\text{-}18}$ in egg PC vesicles. This shift implies that the $C_{18\text{-}18}$ molecule, which has two long alkyl chains, interacts preferentially with the egg PC molecules, measuring the microenvironments in the close vicinity of the egg PC molecules. The η_{eff} value first decreases to a minimum value (about 20 cP), which is still larger than η_{eff} in egg PC vesicles, then increases monotonously toward the mixed micelle-vesicle phase boundary (the broken line in Fig. 5).

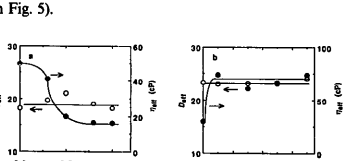

Fig. 6. Effects of cholesterol incorporation on microenvironments surrounding $C_{18\text{-}18}$. $C_{18\text{-}18}$ (0.5 μM) was solubilized in (a) sodium taurocholate micelles (30 mM) and (b) taurocholate/egg PC mixed micelles (the concentrations of egg PC and taurocholate were 13.3 mM and 16.7 mM, respectively) containing various amounts of cholesterol in the buffer at 25°C. Estimated effective dielectric constant (D_{eff}, open circles) and effective viscosity (η_{eff}, closed circles) are shown as a function of the molar percentage of incorporated cholesterol.

$C_{18\text{-}18}$ in sodium taurocholate / cholesterol and sodium taurocholate / egg PC / cholesterol micelles

Fig. 6a shows the effects of cholesterol incorporation on the microenvironments of $C_{18\text{-}18}$ in sodium cholate micelles. The micropolarity does not change on addition of cholesterol up to 1 mol%, near the solubilization limit [23]. On the other hand, the microviscosity decreases significantly, that is, cholesterol fluidizes the micellar interior. Contrary to this, solubilized cholesterol rigidifies sodium taurocholate/egg PC mixed micelles as shown in Fig. 6b. Here the micropolarity remains unaltered on addition of cholesterol.

Discussion

Molecular assemblies formed by amphiphiles, such as micelles and vesicles, provide regions of different microscopic polarities and viscosities. Such microscopic environments or microenvironments have been extensively studied by comparison of the spectral characteristics of incorporated probe molecules with those in reference solvents [17–21,24–29]. Estimated micropolarities, which are often represented by effective dielectric constants [18–21,26,28], depend on the reference system used. Mukerjee and Cardinal [26] recommended the use of hydrocarbon/π-alkanols/water as reference solvent system because dielectric constants in this system, which are proportional to OH dipole concentration, are related to dipole–dipole and hydrogen-bonding interactions.

The fluorescence vibronic structure of a pyrene monomer depends on solvent dipole moment rather than on medium dielectric constant [17]. However, as mentioned above, the dielectric constants in our solvent system can reflect solute–solvent dipolar interactions. In the bile salt micelles, pyrene experiences fairly apolar environments ($D_{\text{eff}} = 5$–11) compared with those in the typical micelles and vesicles ($D_{\text{eff}} \approx 20$), as shown in Table I. This apparently small difference in the D_{eff} values leads to a large difference in dipolar interactions because the interaction energy is proportional to $(D-1)/(2D+1)$ [30] (D: dielectric constant). Indeed, the I_3/I_1 and I_5/I_1 values change most significantly in a range of $D = 2$–10 (data not shown, see Ref. 17). Similar apolar environments, although roughly estimated, have been suggested for sodium cholate, sodium deoxycholate, and sodium taurochenodeoxycholate micelles [13]. These observations are explained in terms of solubilization of pyrene between steroidal hydrophobic surfaces [12]. Aromatic hydrocarbons such as pyrene in micelles are known to be located primarily at micellar surfaces [31], even if they are attached to the ω carbon of a long chain fatty acid [19]. Their affinity to polar environments is attributed to a hydrophilic character of π-electron systems and to high surface energy of micelles [26]. In this context the observed hydrophobic environments of pyrene bile salt micelles suggest low energy of their surfaces, that is, non-existence of high energy 'cleavages' which aromatic molecules fit to lower the surface energy. The micropolarity difference within the four bile salt micelles investigated (Table I) may be interpreted as partial solubilization of pyrene in 'palisade layers' formed by the side-chains of sodium glycocholate and sodium taurocholate [13].

We have investigated the microenvironments of $C_{18\text{-}18}$ in various micelles and vesicles on the basis of (1) the polarity dependence of $\tilde{\nu}_{\max}$ and (2) the polarity and viscosity dependence of ϕ_f^R [18,21]. The results can be summarized as follows: the micropolarities are similar ($D_{\text{eff}} \approx 20$) in all the micelles and vesicles investigated because the positively charged fluorophore tends to be located at their surface polar regions. On the other hand, the microviscosities vary with individual molecular assemblies. In the micelles the η_{eff} values are in an order of several centipoise, whereas in the vesicles they vary from approx. 10 cP in the liquid crystalline bilayers to approx. 60 cP in the gel bilayer. In the bile salt micelles (Table I), the D_{eff} values are similar to those in the other micelles and vesicles, suggesting the positively charged chromophore interacts with the negatively charged head groups of the bile salt molecules. The fairly high η_{eff} values are comparable with those in the gel-state lipid bilayer. The rigid interior of bile salt micelles has been reported on the basis of the intramicellar excimer formation of pyrene [13], the fluorescence quenching of pyrene [12], fluorescence polarization [12,14] and ESR [14]. The two alkyl chains of $C_{18\text{-}18}$ embedded in the rigid interior can immobilize the fluorophore attached directly to the alkyl moiety. The extremely high value in sodium deoxycholate may be attributed to a large aggregate formed by sodium deoxycholate under our experimental conditions (pH 7.0; [NaCl] 150 mM) [1].

The gradual increase in the D_{eff} values of pyrene in sodium taurocholate with addition of egg PC (Fig. 4) seems to be interpreted as follows. Pyrene solubilized between the hydrophobic surfaces of the sodium taurocholate molecules has a D_{eff} of 11, whereas pyrene surrounded by the egg PC molecules experiences a D_{eff} of 16–17. The observed increase in D_{eff} thus represents the release of pyrene molecules sandwiched between the steroid rings into the phospholipid environment. At an egg PC-to-taurocholate ratio of 0.5, the taurocholate simple micelles disappear and the mixed micelles are the unique species in the solution up to a ratio of about 1.5, where the micelle-to-vesicle transition occurs. The pyrene molecules are, therefore, translocated from the interior of the sodium taurocholate micelles to the boundary between the hydrophobic surfaces of the dimeric taurocholate molecules or peripheral ones in the mixed micelles, and further from the boundary to the egg PC environment of the vesicles. The translocation

suggests that the opportunity of contact between the nonpolar steroidal moieties decreases with increasing egg PC molar fraction.

The microenvironments surrounding C_{18-18} in the mixed micelles were found to change with the egg PC-to-taurocholate molar ratio in a complexed manner (Fig. 5). In the presence of egg PC C_{18-18} seems to interact preferentially with the egg PC molecules as suggested by the finding that the D_{eff} values decrease upon addition of a small amount of egg PC, with no further change upon addition of more egg PC. Accordingly, the microviscosities of C_{18-18} are related to the assembly states of the egg PC molecules. The initial reduction of microviscosity is due to the translation of C_{18-18} from the sodium cholate micellar interior to the neighbor of egg PC. Further addition of egg PC causes the rise in η_{eff} ascribed to an increased size of the mixed micelles [7,8]. Such a tight phospholipid packing has been reported by using a deutrium NMR technique [9]. Furthermore, the maximum microviscosity has been detected in the region of the micelle/vesicle phase boundary on the basis of diphenylhexatriene fluorescence polarization [15] and 1,3-diphenylpropane excimer formation [16].

Cholesterol incorporation into sodium cholate micelles fluidizes the micellar interior (Fig. 6a). This effect coincides with an earlier observation that cholesterol enhances the permeability of small molecules into the micelle [12]. In contrast, solubilized cholesterol in the sodium taurocholate/egg PC mixed micelles seems to induce a tighter packing of the egg PC molecules (Fig. 6b). A similar cholesterol effect has been observed in egg PC bilayers [32]. The results suggest preferential interactions of egg PC–C_{18-18} and egg PC–cholesterol in the mixed micelles.

Conclusions

The micropolarities and the microviscosities in the close vicinity of pyrene or C_{18-18} solubilized in the bile salt/egg PC systems are correlated with the structural change of the mixed-lipid assemblies in aqueous media. The bile salt micelles are characterized by a rigid and nonpolar interior. In sodium taurocholate/egg PC mixed micelles, the egg PC molecules are motionally restricted compared with those in egg PC vesicles. Cholesterol incorporation causes fluidization of sodium taurocholate micellar interior, but immobilization of the egg PC molecules in the mixed micelles.

References

1 Carey, M.C. and Small, D.M. (1972) Arch. Intern. Med. 130, 506–527.
2 Mazer, N.A., Carey, M.C., Kwasnick, R.F. and Benedek, G.B. (1979) Biochemistry 18, 3064–3075.
3 Roda, A., Hofmann, A.F. and Mysels, K.J. (1983) J. Biol. Chem. 258, 6362–6370.
4 Schurtenberger, P., Mazer, N. and Känzig, W. (1983) J. Phys. Chem. 87, 308–315.
5 Mukerjee, P., Moroi, Y., Murata, M. and Yang, A.Y.S. (1984) Hepatology 4, 61S–65S.
6 Müller, K. (1981) Biochemistry 20, 404–414.
7 Mazer, N.A., Benedek, G.B. and Carey, M.C. (1980) Biochemistry 19, 601–615.
8 Schurtenberger, P., Mazer, N. and Känzig, W. (1985) J. Phys. Chem. 89, 1042–1049.
9 Stark, R.E., Manstein, J.L., Curatol, W. and Sears, B. (1983) Biochemistry 22, 2486–2490.
10 Spink, C.H., Müller, K. and Sturtevant, J.M. (1982) Biochemistry 21, 6598–6605.
11 Almog, S., Kushnir, T., Nir, S. and Lichtenberg, D. (1986) Biochemistry 25, 2597–2605.
12 Chen, M., Grätzel, M. and Thomas, J.K. (1975) J. Am. Chem. Soc. 97, 2052–2057.
13 Zana, R. and Guveli, D. (1985) J. Phys. Chem. 89, 1687–1690.
14 Fisher, L. and Oakenfull, D. (1979) Aust. J. Chem. 32, 31–39.
15 Schubert, R., Beyer, K., Wolburg, H. and Schmidt, K.-H. (1986) Biochemistry 25, 5263–5269.
16 Reda, F. and Spink, C. (1987) J. Phys. Chem. 91, 1628–1634.
17 Kalyanasundaram, K. and Thomas, J.K. (1977) J. Am. Chem. Soc. 99, 2039–2044.
18 Handa, T., Komatsu, H., Matsuzaki, K. and Nakagaki, M. (1984) Nippon Kagaku Kaishi, 8–13.
19 Handa, T., Matsuzaki, K. and Nakagaki, M. (1987) J. Colloid Interface Sci. 116, 50–58.
20 Mukerjee, P. and Ray, A. (1966) J. Phys. Chem. 70, 2144–2149.
21 Nakagaki, M., Komatsu, H. and Handa, T. (1986) Chem. Pharm. Bull. 34, 4486–4493.
22 West, W. and Pearce, S. (1965) J. Phys. Chem. 69, 1894–1903.
23 Mazer, N.A. and Carey, M.C. (1983) Biochemistry 22, 426–442.
24 Pownall, H.J. and Smith, L.C. (1973) J. Am. Chem. Soc. 95, 3136–3140.
25 Cogan, U., Shinitzky, M., Weber, G. and Nishida, T. (1973) Biochemistry 12, 521–528.
26 Mukerjee, P. and Cardinal, J.R. (1978) J. Phys. Chem. 82, 1620–1627.
27 Zachariasse, K.A., Van Phuc, N. and Kozankiewicz, B. (1981) J. Phys. Chem. 85, 2676–2683.
28 Ramachandran, C., Pyter, R.A. and Mukerjee, P. (1982) J. Phys. Chem. 86, 3198–3205.
29 Handa, T., Ichihashi, C., Yamamoto, I. and Nakagaki, M. (1983) Bull. Chem. Soc. Jpn. 56, 2548–2554.
30 Mataga, N. and Kubota, T. (1970) Molecular Interactions and Electronic Spectra, pp. 371–410, Marcel-Dekker, New York.
31 Ganesh, K.N., Mitra, P. and Balasubramanian, B. (1982) J. Phys. Chem. 86, 4291–4293.
32 Schreier-Muccillo, S., Marsh, D., Dugas, H., Schneider, H. and Smith, I.C.P. (1973) Chem. Phys. Lipids 10, 11–27.